ELSEVIER

Nuclear Instruments and Methods in Physics Research A 441 (2000) 183–190

NUCLEAR INSTRUMENTS & METHODS IN PHYSICS RESEARCH Section A

www.elsevier.nl/locate/nima

Recombination in electron coolers

A. Wolf[a,*], G. Gwinner[a], J. Linkemann[a], A.A. Saghiri[a], M. Schmitt[a], D. Schwalm[a], M. Grieser[a], M. Beutelspacher[a], T. Bartsch[b], C. Brandau[b], A. Hoffknecht[b], A. Müller[b], S. Schippers[b], O. Uwira[b], D.W. Savin[c]

[a]*Max-Planck-Institut für Kernphysik, Heidelberg and Physikalisches Institut der Universität, Postfach 103980, D-69029 Heidelberg, Germany*
[b]*University of Giessen, Germany*
[c]*Columbia University, NY, USA*

Abstract

An introduction to electron–ion recombination processes is given and recent measurements are described as examples, focusing on low collision energies. Discussed in particular are fine-structure-mediated dielectronic recombination of fluorine-like ions, the moderate recombination enhancement by factors of typically 1.5–4 found for most ion species at relative electron–ion energies below about 10 meV, and the much larger enhancement occurring for specific highly charged ions of complex electronic structure, apparently caused by low-energy dielectronic recombination resonances. Recent experiments revealing dielectronic resonances with very large natural width are also described.

PACS: 29.20.Dh; 34.80.Lx

Keywords: Radioactive recombination; Dielectronic recombination; Electron cooling

1. Introduction

Electron–ion recombination leads to loss of stored positive ions during electron cooling, in particular at high ion charge and high beam velocity when rest gas processes become less important. On the other hand, ion storage rings with electron coolers are powerful tools for the experimental study of electron–ion collision processes at well-controlled relative energy.

Spontaneous recombination of electrons and protons was already observed in the first tests of electron cooling [1] and in several electron cooling experiments the shape of the emerging fast atomic hydrogen beam was used as a diagnostic for the angular divergence of the stored proton beam. Also theoretical predictions for radiative recombination of cooling electrons with cooled protons were developed [2] in the context of early electron cooling activities. This happened widely unnoticed by the atomic and molecular physics community; in fact, low-energy single-pass merged beams experiments at the same time just started to measure the much higher rates due to dissociative recombination of molecules [3], while radiative recombination of atomic ions was considered almost undetectable. In the 1980s a small number of single-pass crossed or merged beams experiments succeeded in detecting

* Corresponding author.
E-mail address: a.wolf@mpi-hd.mpg.de (A. Wolf)

0168-9002/00/$ - see front matter
PII: S0168-9002(99)01131-6

dielectronic recombination, a resonant type of radiative recombination, occurring for incompletely stripped atomic ions and having large importance for plasma-physical applications (see reviews by Dunn et al. [4]). These experiments faced large problems from a low signal to background ratio and an often very limited energy resolution. Much improved single-pass arrangements for low-energy recombination measurements could finally be realized by using an electron beam similar to that in electron coolers in Aarhus [5] and a specially designed cold dense electron target at the GSI [6].

However, it was only after heavy-ion storage rings went in operation that recombination processes of atomic ions became accessible for precision experiments. High-resolution measurements on dielectronic recombination began with a study of hydrogenlike ions, in particular O^{7+} [7], at the TSR in Heidelberg, taking particular advantage of the high-current stored ion beam. Many experiments followed at several storage rings on a number of atomic systems; a useful summary of results until 1995 is given in Ref. [8] and more recent results are summarized in Refs. [9,10].

In most of the detailed measurements performed so far, the recombination rates during electron cooling were found to exceed significantly the predictions for radiative recombination. Except for some ions with complex electronic structure, where dielectronic recombination additionally complicates the situation, the enhancement was shown to occur only at very low relative energy and to remain limited to moderate factors of up to ~ 5. Low-energy dielectronic resonances, on the other hand, can much more strongly enhance the recombination rate in particular cases. The present knowledge about the enhanced recombination rates will be discussed below after a short summary of the basic recombination processes and the methods for their experimental study.

2. Recombination processes and experimental procedures

At low electron densities, as encountered in the electron cooling arrangement, recombination between electrons and atomic ions largely proceeds through the capture of a single electron on an ion under emission of a photon. Usually, the non-resonant direct process

$$A^{q+} + e^- \rightarrow A^{(q-1)+} + h\nu \tag{1}$$

is called radiative recombination (RR). The same net effect also results from a resonant reaction via an intermediate doubly excited state $[A^{(q-1)+}]^{**}$,

$$A^{q+} + e^- \leftrightarrow [A^{(q-1)+}]^{**} \rightarrow A^{(q-1)+} + h\nu \tag{2}$$

this two-step process is called dielectronic recombination (DR).

In RR, the incident electron is captured into a Rydberg level n with a cross-section given as a function of the electron energy E in the electron–ion center-of-mass (c.m.) frame by [11,12]

$$\sigma_n(E) = \frac{32\pi}{3\sqrt{3}}\alpha^3 a_B^2 \frac{q^4 R_\infty^2}{nE(q^2 R_\infty + n^2 E)} \tag{3}$$

where $R_\infty \approx 13.6$ eV is the Rydberg energy, a_B the Bohr radius, q the initial ion charge and α the fine structure constant. For small energies $E \ll q^2 R_\infty / n^2$ the cross-section varies as $\propto (nE)^{-1}$; this implies for recombination during electron cooling (i.e. low E) that the contributions from capture into highly excited Rydberg states decrease quite slowly as n increases. Eq. (3) represents in fact the semiclassical result for recombination into hydrogenic (single-electron) states; the obtained cross-sections $\sigma_n(E)$, however, lie close to the exact quantum mechanical results, which at near-zero energy are lower by 20% for $n = 1$ and by much smaller relative amounts for high Rydberg states (see, e.g. Ref. [13]). Since the Rydberg states, taken together, give a large relative contribution to the total rate, the semiclassical formula yields a reasonable approximation even for recombination on ions with electrons already bound, provided the occupied shells are not counted in the sum over the final states.

The recombination rate during electron cooling is obtained as

$$R = \gamma^{-2} \eta_L N_i n_e \alpha_r \tag{4}$$

where N_i is the ion number in the circulating beam, n_e the electron density, η_L the ring fraction occupied by the electron beam, and γ the relativistic factor (n_e and R being defined in the laboratory

frame). The rate coefficient α_r represents the quantity $\langle v\sigma(E)\rangle$, where v is the velocity in the c.m. frame and σ the cross-section summed over all final states; an average denoted by $\langle\ \rangle$ is performed over the velocity distribution in the c.m. frame. Bell and Bell [2] have calculated rate coefficients α_{RR} for radiative recombination in the case of *velocity matched* beams (during electron cooling), assuming a "flattened" velocity distribution of the electrons characterized by the transverse temperature $T_\perp$ and a much smaller longitudinal temperature $T_{||} \ll T_\perp$; they obtained

$$\alpha_{RR} = 3.02\times10^{-13}\frac{\mathrm{cm}^3}{\mathrm{s}}q^2\sqrt{\frac{\mathrm{eV}}{kT_\perp}} \times\left[\ln\left(\frac{11.32q}{\sqrt{kT_\perp/\mathrm{eV}}}\right)+0.14\left(\frac{kT_\perp}{q^2\mathrm{eV}}\right)^{1/3}\right]. \quad (5)$$

The first term in the large brackets can be interpreted as the sum over Rydberg-state capture rates scaling as $\propto 1/n$ (cf. Eq. (3)). The value of this sum logarithmically increases with the maximum quantum number n_{max} of the included final states. From Eq. (3), the Rydberg-state contributions for increasing n are expected to decrease faster than $\propto 1/n$ as soon as the binding energies of the final states n become $\lesssim kT_\perp$; accordingly, the result of Eq. (5) implies that the sum extends up to $n_{max} = 9.53q(kT_\perp/\mathrm{eV})^{-1/2} - 1$, which indicates the highest quantum number of Rydberg states that significantly contribute to the recombination rate. For the typical conditions of electron cooling with $kT_\perp \lesssim 0.1$ eV, n_{max} becomes rather large ($\gtrsim 30q$); moreover, the second term in the large brackets then can be neglected.

As shown in Fig. 1 recombined ions, after leaving the electron cooler, are separated from the circulating beam in the next ring dipole and can be counted on a detector. Ions recombining into high Rydberg states may be field ionized in this ring dipole by motional electric fields, provided they do not decay radiatively to lower states before reaching the dipole. For an approximate description, a cutoff quantum number n_c is introduced, giving the highest final state n for which recombination can be detected. It turns out that $n_c < n_{max}$ in most cases; hence, the sum over Rydberg-state cross-sections scaling as $\propto 1/n$ has to be cut off already at n_c in order to obtain the measured recombination rate. The first term in the large brackets of Eq. (5) then should be replaced by $0.17 + \ln(n_c + 1)$ [14]. From considerations of field ionization it follows that the cutoff quantum number at fixed electric field strength scales approximately as $n_c \propto q^{3/4}$.

During electron cooling there is no average relative motion between electrons and ions; however, by detuning the electron energy and keeping the ion energy fixed, a longitudinal average relative velocity between the beams can be generated. Scanning the electron acceleration voltage, energy-dependent recombination cross-sections of stored ions are measured. The energy corresponding to the velocity detuning is denoted as "relative energy" $\hat{E}$; if it becomes large compared to the electron temperature ($\hat{E} \gg kT_\perp$) it essentially determines the c.m. energy and the observed recombination rate coefficient represents the recombination cross-section folded with the c.m. electron energy spread and multiplied by the relative velocity: $\alpha_r(\hat{E}) \approx \hat{v}\langle\sigma(\hat{E})\rangle$. The rate coefficient for RR will then scale roughly

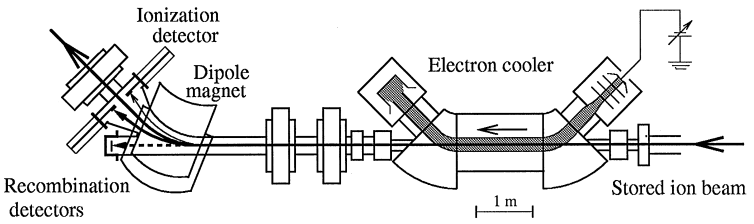

Fig. 1. Schematic drawing of the electron cooling section of the heavy ion storage ring TSR, showing the path of the stored ion beam, the cooling device, and the detectors for recombined ions (or neutrals in the case of singly charged stored ions). On an additional detector electron impact ionization rates can be measured.

as $\propto \hat{E}^{-1/2}$, corresponding to the E^{-1} dependence of the cross-section; any DR resonances will appear on top of this continuous recombination signal. Experimental aspects of DR measurements at different storage rings are explained in more detail in Refs. [15,16] for the TSR, in Ref. [17] for TARN, and in Ref. [18] for CRYRING; measurements for the heaviest few-electron systems (U^{89+} at GSI) are reported in Ref. [19]. Further methods of atomic physics experiments at heavy-ion storage rings are summarized in Ref. [20].

3. Dielectronic recombination spectra

As an example for a typical dielectronic recombination spectrum recently investigated [21,22], we will consider the fluorine-like ion Fe^{17+}. Starting with the given ground-state configuration of Fe^{17+}, an intermediate doubly excited state $[A^{(q-1)+}]^{**}$ is formed when a free electron excites a 2s electron to 2p and is simultaneously captured into an nl Rydberg state,

$$Fe^{17+}[2s^2(2p^5)_{3/2}] + e^- \leftrightarrow Fe^{16+}(2s2p^6\,nl) \quad (n = 6, \ldots, \infty). \tag{6}$$

The capture is reversible since the doubly excited state can autoionize again; however, it can also decay radiatively,

$$Fe^{16+}(2s2p^6\,nl) \rightarrow Fe^{16+}(2s^22p^5nl) + h\nu \tag{7}$$

which completes DR. In addition to this conventional DR process, also a more exotic excitation mechanism can occur in fluorine-like systems (as first observed on the isoelectronic ion Se^{25+} [16]). Here, spin recoupling in the 2p shell is induced by the colliding electron which is also captured in a Rydberg state:

$$Fe^{17+}[2s^2(2p^5)_{3/2}] + e^- \leftrightarrow Fe^{16+}[2s^2(2p^5)_{1/2}nl\,] \quad (n = 18, \ldots, \infty) \tag{8}$$

thus, a fine-structure excitation of the one-hole configuration $2p^5$ occurs, changing its total angular momentum from $\frac{3}{2}$ to $\frac{1}{2}$. A radiative transition of the Rydberg electron to a level below the ionization threshold ($n' < 18$) completes this DR:

$$Fe^{16+}[2s^2(2p^5)_{1/2}nl\,] \rightarrow Fe^{16+}[2s^2(2p^5)_{1/2}n'l'] + h\nu \tag{9}$$

the other possibility, a radiative decay of the fine-structure excited $(2p^5)_{1/2}$ configuration back to $(2p^5)_{3/2}$, is much less probable as it is electric dipole forbidden. Rydberg series originating from both types of DR processes can be seen in the measured spectrum (Fig. 2). The channel of fine-structure-mediated DR, as represented by the series of low-energy resonances up to $\sim$13 eV, has been ignored in the past by modelers of cosmic plasmas for Fe^{17+} and similar ions. Its inclusion considerably changes the DR rates needed to understand the structure of X-ray photoionized cosmic plasmas [21,22].

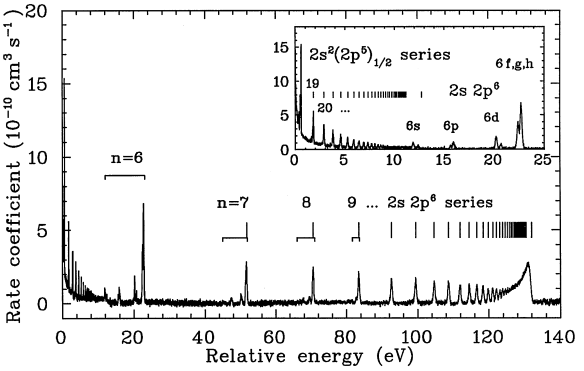

Fig. 2. Recombination rate coefficient of Fe^{17+} ions stored in the TSR at 5.6 MeV/u, measured [21,22] as a function of the relative energy $\hat{E}$. On top of the continuous RR signal the series of DR resonances $2s2p^6\,nl$ for $n \geqslant 6$ (with resolved fine structure for $n = 6$–8) is seen; levels with up to $n_c \approx 124$ are estimated to contribute to the Rydberg peak with a series limit at 132 eV. At lower energies (see also the inset) fine-structure-mediated DR causes additional recombination via $2s^2(2p^5)_{1/2}\,nl$ resonances.

4. Recombination at low relative energies

Recombination rates at low relative energies were studied both in single-pass arrangements and in storage rings. In the early electron cooling

experiments with protons, no deviations from theoretical predictions were found with regard to the RR rates. However, a measurement [6,23] on the complex heavy ion U^{28+} at the GSI single-pass electron target, first performed in 1989, showed extremely high recombination rates at matched beam velocities, which exceeded predictions for RR by a factor of ~ 200. Such recombination rates during electron cooling would lead to beam lifetimes of only a few seconds for U^{28+} ions in a storage ring. On the other hand, at about the same time electron cooling of heavy ions (first on C^{6+}) was realized in ion storage rings [24,25], yielding beam lifetimes as long as predicted and thus confirming the RR theory within a factor of ~ 2. Moreover, in measurements [13,26] at the Aarhus single-pass electron target, radiative recombination rates for ions such as C^{6+} were measured with $\sim 20\%$ accuracy at energies up to 1 eV, yielding agreement with the RR theory. Thus, the excess rates found for U^{28+} could appear as an exception, possibly caused by the complicated electronic structure of this ion.

Nevertheless, discrepancies between theory and experiment were found also for ions with much simpler structure (and later even for bare ions) when recombination rates were directly measured in merged beams at relative energies below ~ 10 meV, which could not be well controlled at the Aarhus single-pass target. First, observations of such discrepancies were made at GSI, using the cold dense single-pass electron target, in measurements on Ar^{15+} ions [27]; they showed agreement with the predicted RR rate at energies of $\gtrsim 10$ meV, but at lower energies an unexpected rise of the measured rate by a factor of ~ 4 occurred, forming a sharp "cusp" peak around zero relative beam velocity. An example of the characteristic energy dependence of this enhancement phenomenon can be seen in Fig. 3(c). A remarkable property of the sharp cusp peak is that it rises at relative energies considerably below the transverse thermal electron energy ($kT_\perp$); hence, the matching of the *longitudinal* velocities of electrons and ions (limited by $kT_{||}$ which is much smaller than $kT_\perp$) seems to be important for obtaining the recombination enhancement.

Directly measured recombination rates of highly charged ions during electron cooling at the TSR

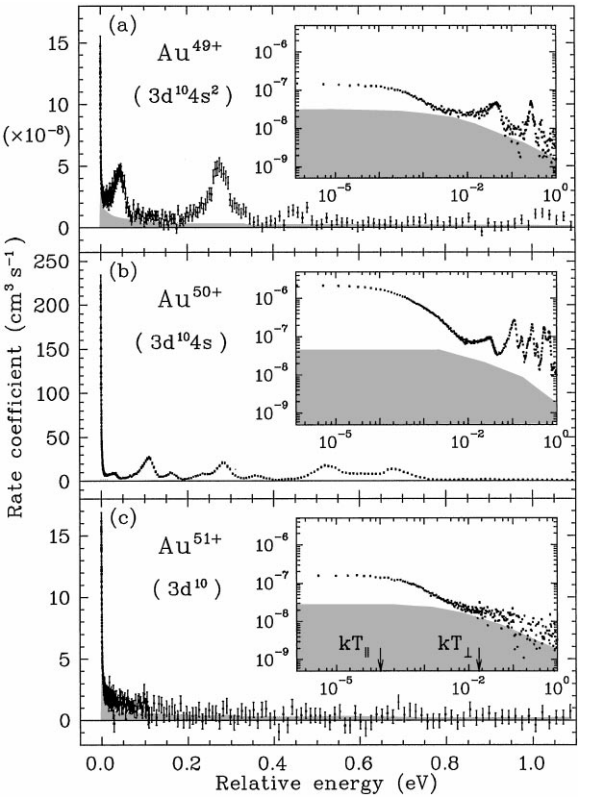

Fig. 3. Recombination rate coefficient of highly charged Au ions with the given charge states and configurations stored in the TSR at 3.6 MeV/u, measured [35] as a function of the relative energy $\hat{E}$. No detailed assignment of the DR resonances for Au^{49+} and Au^{50+} has been obtained. The theoretical RR rate coefficients (shaded areas) were calculated from the cross-section of Eq. (3), summing over the electron shells open for recombination (Rydberg-state detection limit $n_c = 360$).

since ~ 1990 also indicated an enhancement of the low-energy recombination rate. First, for C^{6+} and Cl^{17+} ions, recombination rates too high to be reconciled with the RR cross-section and the expected field ionization of high Rydberg states were found [28]; in the following, enhancement factors of 1.3–1.7 were observed for a number of bare and few-electron ions up to $q = 26$ [15,16,29,30]. An energy dependence equivalent to the one seen at the GSI single-pass target was established for the enhanced recombination rates at storage rings by measurements at CRYRING [31]. As a general trend, the recombination rates in the magnetized

electron beams used for electron cooling are fairly well reproduced by the theoretical predictions for RR at relative energies above a few meV, but the additional rise of the rate at even lower energies – with an increase of the total rate by typical factors of 1.5–4 – has not been explained theoretically so far. This moderate low-energy enhancement does not appear to depend on details of the electronic structure of the recombining ions. It might be related to general properties of the interaction of cold magnetized electrons with ions at small relative velocities, as it occurs in the magnetically guided electron beam of the electron cooler and was considered for example in Ref. [32]. Investigations regarding the dependence of the enhancement on experimental parameters such as the electron density, the ion charge, and external fields in the electron cooler are underway. A more detailed discussion is given in Ref. [33].

5. Low-energy dielectronic resonances

A number of other cases with very large low-energy recombination enhancement have been discovered among more complex atomic ions. At LEAR, operating with lead ions Pb^{q+}, $q = 52$–54, an anomalously short beam lifetime of only ~ 8 s was observed [34] during electron cooling of Pb^{53+}, while the lifetimes for Pb^{52+} and Pb^{54+} (~ 40–50 s) were close to the predictions. The strong dependence of the Pb^{53+} lifetime on the electron beam current indicated that the loss was caused by recombination. Direct measurements of the recombination rate were performed at the TSR for ions isoelectronic to these systems with similar nuclear charge (Au^{q+}, $q = 49$–51) [35]. The ion energy was close to 3.6 MeV/u, the electron density amounted to $\sim 1 \times 10^7$ cm^{-3}, and the electron temperatures were $kT_\perp = 16$ meV and $kT_{||} \approx 0.1$ meV. The scans of the relative energy $\hat{E}$ were extended up to ~ 1 eV, yielding the results shown in Fig. 3. For all charge states, a significant rise of the recombination rate, starting when $\hat{E}$ becomes lower than ~ 5–8 meV, is found. Moderate enhancement factors of ~ 5 as compared to the calculated RR are found for Au^{49+} and Au^{51+}, while the recombination rate coefficient for Au^{50+} is extremely high (up to $\sim 2 \times 10^{-6}$ cm^3 s^{-1} at $\hat{E} = 0$) and the enhancement factor with respect to RR theory amounts to ~ 60. Note that the respective isoelectronic pairs of Au^{q+} and Pb^{q+} ions investigated at the TSR and at LEAR seem to behave very similar to each other as concerns the recombination rate. The recombination spectra for the three Au^{q+} ions (Fig. 3) suggest a strong influence of low-energy DR resonances on the zero-energy recombination rate of Au^{50+}; many such resonances are observed for this ion, whereas only a few resonances are seen for Au^{49+} and none for Au^{51+}. For Au^{50+} the recombination rate is considerably larger than predicted for RR at all energies in the scan range, while for the other ions it is reasonably well reproduced by the calculated RR rate. A detailed assignment of the observed resonances would require highly accurate atomic structure calculations which presently are not available for this system. More general theoretical work regarding electron recombination with complex ions [36] has been motivated by the observations of large enhancement factors but, at least at its present state, cannot be used to obtain predictions for the detailed influences of the electronic structure, as found in the experiments.

A recent recombination experiment on atomic ions with another complex electron configuration sheds additional light on the mechanism by which low-energy DR resonances can enhance the recombination rate during electron cooling. In particular, low-energy resonances can contribute significantly to the total recombination cross-section near $E = 0$ when their *natural width* is larger than or of the order of the resonance energy. Large natural widths can result from rapid autoionization. In the Ar-like ion Ti^{4+} studied at the TSR [37], dielectronic capture can proceed via

$$Ti^{4+}(3p^6) + e^- \leftrightarrow Ti^{3+}(3p^5 3d\,nl) \qquad (10)$$

terms of the configuration $Ti^{3+}(3p^5 3d^2)$ are expected to autoionize back to $Ti^{4+}(3p^6) + e^-$ very rapidly, since for this decay the two electrons in the initial state and the bound electron in the final state all reside in the same electronic shell. Ab initio calculations using a standard atomic structure code predict the ^{2}F term of this configuration to have a particularly large natural width of ~ 1.3 eV. In the experimental recombination spectrum (Fig. 4)

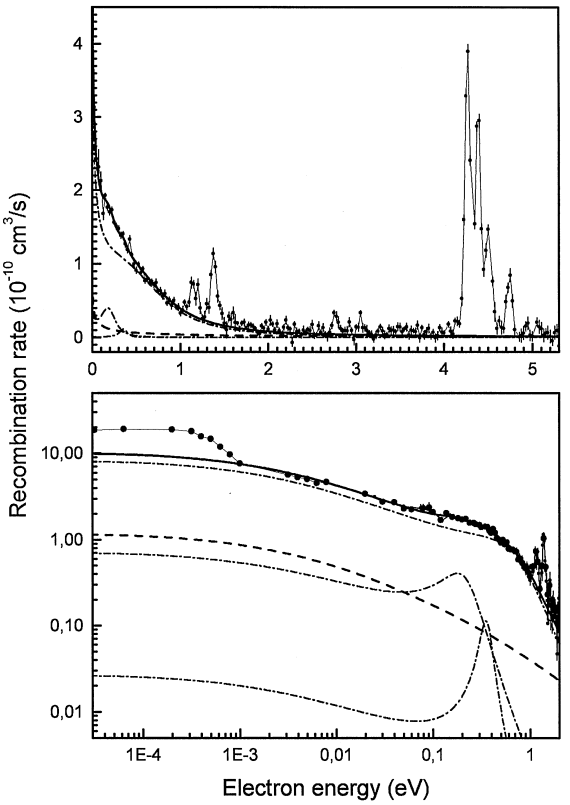

Fig. 4. Recombination rate coefficient of Ti^{4+} ions stored in the TSR at 0.6 MeV/u, measured [37] as a function of the relative energy $\hat{E}$ (experimental energy spread (FWHM) ~ 0.06 at 4 eV and $\lesssim 0.03$ at $\leqslant 1$ eV). Narrow DR resonances (presumably with configurations $3p^5 3d\,4l$) and a strong wide resonance at near-zero energy (identified as $3p^5 3d^2\ ^2F$) are observed. Dashed line: calculated RR rate coefficient (Rydberg-state detection limit $n_c = 30$), yielding only $\sim 5\%$ of the total rate at $\hat{E} = 0$; dash-dotted lines: DR signals from the strong near-threshold resonance with a fitted width of 1.2 eV and a position of 0.45 eV (uppermost line) and from further small resonances (peak positions 0.2 and 0.36 eV, natural widths 0.2 and 0.1 eV). The lower panel also shows the enhancement at $\hat{E} \lesssim 1$ meV as discussed in Section 4.

a strong and wide resonance can in fact be indentified by fitting the spectral shape. The fit parameters result in a centroid of 0.45 eV and a width of 1.2 eV, and the resonance is attributed to the $3p^5 3d^2\ ^2F$ term based on a comparison with the ab initio calculation, which provides some guidance in spite of its limited accuracy for such complex configurations.

The observed recombination rate at $\hat{E} = 0$ exceeds the predicted RR rate by a factor of ~ 20. At very low relative energy (here when $\hat{E}$ becomes lower than ~ 1 meV), again the typical rise of the total rate by a moderate factor occurs; however, even at higher energies the observed rate exceeds the RR calculation by a factor of ~ 10. As shown in Fig. 4, the rate coefficients for three DR resonances were added to the calculated RR rate coefficient and the total rate was fitted to the experimental signal above 2 meV, varying the DR resonance parameters. In fact, the broad resonance at 0.45 eV accounts for most of the observed signal; the two weaker resonances only improve the fit around 0.2 eV.

In summary, all experimental evidence indicates that the strong enhancement of recombination rates during electron cooling found for certain complex highly charged ions is caused by low-energy dielectronic resonances. A recent experiment in particular shows that such resonances can have a very large natural width, which can bring a considerable part of their strength to zero collision energy without sharp requirements on the exact resonance position. The existence or absence of DR resonances that would boost the low-energy recombination rate cannot safely be predicted for each and every ion by theoretical means and therefore can be established only by experimental tests or direct recombination measurements.

Acknowledgements

This work was supported in part by the German Federal Minister for Education and Research (BMBF) through contracts 06 GI 848 and 06 HD 854 and by the HCM Program of the European Community.

References

[1] G.I. Budker, N.S. Dikansky, V.I. Kudelainen, I.N. Meshkov, V.V. Parkhomchuk, A.N. Skrinsky, B.N. Sukhina, Part. Accel. 7 (1976) 197.
[2] M. Bell, J.S. Bell, Part. Accel. 12 (1982) 49.
[3] D. Auerbach, R. Cacak, R. Caudano, T.D. Gaily, C.J. Keyser, J.Wm. McGowan, J.B.A. Mitchell, S.F.J. Wilk, J. Phys. B 10 (1977) 3797.

[4] G.H. Dunn, P.F. Dittner, S. Datz, in: W.G. Graham, W. Fritsch, Y. Hahn, J.A. Tanis (Eds.), Recombination of Atomic Ions, NATO ASI Series B: Physics, Vol. 296, Plenum Press, New York, 1992.
[5] L.H. Andersen, P. Hvelplund, H. Knudsen, P. Kvistgaard, Phys. Rev. Lett. 62 (1989) 2656.
[6] A. Müller, S. Schennach, M. Wagner, J. Haselbauer, O. Uwira, W. Spies, E. Jennewein, R. Becker, M. Kleinod, U. Pröbstel, N. Angert, J. Klabunde, P.H. Mokler, P. Spädtke, B. Wolf, Phys. Scripta T37 (1991) 62.
[7] G. Kilgus et al., Phys. Rev. Lett. 64 (1990) 737.
[8] M. Larsson, Rep. Progr. Phys. 58 (1995) 1267.
[9] A. Müller, in: H.F. Beyer, V.P. Shevelko (Eds.), Atomic Physics with Heavy Ions, Springer, Berlin, 1999 (Chapter XII).
[10] S. Schippers, Phys. Scripta T80 (1999) 158.
[11] H.A. Bethe, E.E. Salpeter, Quantum Mechanics of One- and Two-Electron Systems, Plenum Press, New York, 1977, p. 322.
[12] H.A. Kramers, Philos. Mag. 46 (1923) 836.
[13] L.H. Andersen, J. Bolko, Phys. Rev. A 42 (1990) 1184.
[14] A. Wolf, in: W.G. Graham, W. Fritsch, Y. Hahn, J.A. Tanis (Eds.), Recombination of Atomic Ions, NATO ASI Series B: Physics, Vol. 296, Plenum Press, New York, 1992.
[15] G. Kilgus, D. Habs, D. Schwalm, A. Wolf, N.R. Badnell, A. Müller, Phys. Rev. A 46 (1992) 5730.
[16] A. Lampert, A. Wolf, D. Habs, J. Kenntner, G. Kilgus, D. Schwalm, M.S. Pindzola, N.R. Badnell, Phys. Rev. A 53 (1996) 1413.
[17] T. Tanabe, M. Tomizawa, K. Chida, T. Watanabe, S. Watanabe, M. Yoshizawa, H. Muto, K. Noda, M. Kanazawa, A. Ando, A. Noda, Phys. Rev. A 45 (1992) 276.
[18] W. Zong, R. Schuch, E. Lindroth, H. Gao, D.R. DeWitt, S. Asp, H. Danared, Phys. Rev. A 56 (1997) 386.
[19] C. Brandau, F. Bosch, G. Dunn, B. Franzke, A. Hoffknecht, C. Kozhuharov, P.H. Mokler, A. Müller, F. Nolden, S. Schippers, Z. Stachura, M. Steck, T. Stöhlker, T. Winkler, A. Wolf, Hyperfine Interactions 114 (1998) 45.
[20] A. Wolf, in: H.F. Beyer, V.P. Shevelko (Eds.), Atomic Physics with Heavy Ions, Springer, Berlin, 1999 (Chapter I).
[21] D.W. Savin, T. Bartsch, M.H. Chen, S.M. Kahn, D.A. Liedahl, J. Linkemann, A. Müller, S. Schippers, M. Schmitt, D. Schwalm, A. Wolf, Astrophys. J. Lett. 489 (1997) L115.
[22] D.W. Savin, S.M. Kahn, J. Linkemann, A.A. Saghiri, M. Schmitt, M. Grieser, R. Repnow, D. Schwalm, A. Wolf. T. Bartsch, C. Brandau, A. Hoffknecht, A. Müller, S. Schippers, M.H. Chen, N.R. Badnell, Astrophys. J. Suppl. Ser. 123 (1999) 687.
[23] O. Uwira, A. Müller, W. Spies, A. Frank, J. Linkemann, L. Empacher, P.H. Mokler, R. Becker, M. Kleinod, S. Ricz, Nucl. Instr. and Meth. B 98 (1995) 162.
[24] D. Krämer et al., Nucl. Instr. and Meth. A 287 (1990) 268.
[25] M. Steck et al., Nucl. Instr. and Meth. A 287 (1990) 324.
[26] L.H. Andersen, J. Bolko, P. Kvistgaard, Phys. Rev. Lett. 64 (1990) 729.
[27] S. Schennach, A. Müller, O. Uwira, J. Haselbauer, W. Spies, A. Frank, M. Wagner, R. Becker, M. Kleinod, E. Jennewein, N. Angert, P.H. Mokler, N.R. Badnell, M.S. Pindzola, Z. Phys. D 30 (1994) 291.
[28] A. Wolf, J. Berger, M. Bock, D. Habs, B. Hochadel, G. Kilgus, G. Neureither, U. Schramm, D. Schwalm, E. Szmola, A. Müller, M. Wagner, R. Schuch, Z. Phys. D 21 (1991) S69.
[29] A. Wolf, in: H. Walther, T.W. Hänsch, B. Neizert (Eds.), Atomic Physics 13, AIP Conference Proceedings, Vol. 275, AIP, New York, 1993, p. 228.
[30] U. Schramm, T. Schüssler, D. Habs, D. Schwalm, A. Wolf, Hyperfine Interactions 99 (1996) 309.
[31] H. Gao, D.R. DeWitt, R. Schuch, W. Zong, S. Asp, M. Pajek, Phys. Rev. Lett. 75 (1995) 4381.
[32] G. Zwicknagel, Q. Spreiter, C. Toepffer, Hyperfine Interactions 108 (1997) 131.
[33] A. Müller, A. Wolf, Hyperfine Interactions 109 (1997) 233.
[34] S. Baird, J. Bosser, C. Carli, M. Chanel, P. Lefèvre, R. Ley, R. Maccaferri, S. Maury, I. Meshkov, D. Möhl, G. Molinari, F. Motsch, H. Mulder, G. Tranquille, F. Varenne, Phys. Lett. B 361 (1995) 184.
[35] O. Uwira, A. Müller, J. Linkemann, T. Bartsch, C. Brandau, M. Schmitt, A. Wolf, D. Schwalm, R. Schuch, W. Zong, H. Lebius, W.G. Graham, J. Doerfert, D.W. Savin, Hyperfine Interactions 108 (1997) 149.
[36] L. Bureyeva, V. Lisitsa, J. Phys. B 31 (1998) 1477.
[37] S. Schippers, T. Bartsch, C. Brandau, J. Linkemann, G. Gwinner, A. Müller, A.A. Saghiri, A. Wolf, J. Phys. B 31 (1998) 4873.